

New organic dyes based on D - π - A structural sensitizers for Dye-sensitized solar cells (DSSC's): DFT and TD-DFT investigation.

M. YanadiRao¹, G. Ravi Kumar², P. Sumalatha², Sricharitha Annam^{3*}
Mannam SubbaRao⁴,

1 Department of Chemistry, SCIM Government Degree College, Tanuku, W.G. Dist., A.P., India.

2 Department of Chemistry, Government Degree College (Autonomous), Siddipet- 502 103, T.S., India.

3 Department Humanities and Sciences. VNR VignanaJyothi Institute of Enng& Tech, Nizampet, Hyderabad-500090. Telangana, India

4Department of Chemistry, Acharya Nagarjuna University, Guntur-522 510, A.P., India.

* Corresponding author: mannamsrao@gmail.com

Abstract

The present research aims to design the new dyes with a D- π -A structure to apply Dye-sensitized solar cells. The D- π -A dyes constitute S1 to S9, using 9-vinyl-9H-carbazole (D) as a donor (D); different thiophene derivatives are π - spacers and cyanoacrylic acid is an acceptor. For the electronic and optical properties calculation of the studied dyes, use DFT/B3LYP/6-311G++ level of theory by using Gaussian 09W software. Using optimized geometrical structures to calculate the UV absorption spectra, utilize the TD-DFT method in the gas and acetonitrile solvent. The HOMO and LUMO energy gap (Eg) values of S5 and S9 dyes show a narrow band gap with 1.8 eV and 1.7 eV, respectively. So all studied dyes have LUMO values higher than the TiO₂ conduction band and HOMO values lower than the electrolyte redox potential. The UV absorption spectral data shows S5 and S9 have maximum absorption at 759 nm and 803 nm, respectively. So all the studied dyes are suitable for DSSC application.

Keywords: 9-vinyl-9H-carbazole, π -spacer, acceptor, DFT/TD-DFT method, energy gap.

Introduction

One cannot overstate the importance of photovoltaics as a source of energy. The growing worldwide population greatly influences the rising energy demand. While fossil fuels have historically been the most significant energy source, they have drawbacks such as global warming and environmental degradation [1-3]. As a result, solar cell becomes crucial to reducing the risks that fossil fuels provide to the environment and human health. A solar cell is a gadget that uses sunshine to create electricity [4]. The benefits of solar energy include being large-scale, inexpensive, clean, renewable, inexhaustible, and non-polluting [5]. Moreover, solar energy continues to be the primary energy source since the sun contains more than enough energy to last a million years.

Despite this, silicon-based solar cells have yields of between 15% and 25.4% [6]. Both their weight and cost of production are high. This prevents people and manufacturers from using them widely. The (DSSC) or "Gratzel cell," a photoelectrochemical device that transforms sunlight into energy, is a new approach to lower the cost of these cells [7, 8]. Their present

yield is over 13% and they have a design that produces a wide range of molecular structures that are available and sustainable in colour [9-13]. "Due to their adaptability, cheap production costs, and biodegradability, dye-sensitized solar cells (DSSCs) have been the subject of extensive research for almost three decades" [14,15]. A mesoporous oxide semiconductor layer, a transparent conductive glass substrate, a redox electrolyte, a counter electrode, and a dye sensitizer are the five elements that make up a DSSC [16,17]. However, the dye sensitizer significantly impacts the efficiency of light harvesting, stability, charge separation, charge injection, incident light conversion to photocurrent, and overall energy conversion [18-20].

Donors (D), such as triarylamine or carbazole, are found in the most efficient organic dyes (DSSCs), which contain a donor-bridge-acceptor (D- π -A) chemical architecture. Many examples of diverse D- π -A compounds based on the PTZ framework with varied linkers and noteworthy photovoltaic performance can be found in the literature [21-23]. The donor in our investigation is the phenothiazine group (PTZ), while the acceptor is a group generated from cyanoacrylic acid. This push-pull system enables intramolecular charge transfer from the donor group to the acceptor through the conjugated units. Several research teams have worked to enhance the D-A dyes' characteristics in recent years [24].

The absorption of the photosensitizer on the surface of the semiconductor is the fundamental working principle of the dye solar cell. The dye is excited to its initial excited state (S^*) when light (in the visible spectrum) is absorbed. The dye is then oxidized when electrons are transported to the carboxyl groups (COOH) at the ends of the dye's rings, which form bonds with the surface of the TiO_2 network and give it a proton. The dye is then regenerated against the counter electrode after being decreased by a reducing agent [25]. The electron transfer from the dye to TiO_2 and the hole transport from the oxidized dye to the electrolyte processes in the

(DSSC) achieve charge separation. The electronic structure of the absorbing dye molecule and the suitability of the energy levels between the excited state of the dye and the TiO_2 CB strongly influence the electron transfer mechanism.

However, the position of energy levels between the dye molecule and other nanoparticles directly affects charge separation. The excited state S^* of the dye is bigger than TiO_2 's conduction band gap, and its (level 1) chemical potential is lower than the electrolyte's redox iodide/triiodide pair's (I^-/I_3^-) chemical potential [26]. These two currently act as the electron and hole separation's energetic propellers. "The semiconductor nanoparticle array serves as a transport medium for the electrons injected from the dye molecules and serves as a large substrate surface for the molecules. Numerous metal-free organic dyes, such as phenothiazine" [27], carbazoles, coumarin, triarylamine, triphenylamines [28-30], or phenoxazine [31, 32], have been developed and synthesized. It has been discovered that they have promising properties that can improve the performance of photovoltaics. Phenoxazine has recently become a favourite electron-donating residue. Phenoxazine has a greater conversion efficiency than colours based on triphenylamine and phenothiazine, which have a comparable structure, according to Karlsson and colleagues [33].

"Additionally, the adaptability of phenoxazine allows for the reduction of the energy gap through the incorporation of additional donor groups into the residue molecules, which helps to overcome the issues of lower conversion efficiency, narrow absorption spectra, poor stability, and poor photovoltaic properties typical of metal-free organic dyes" [34,35]. Among many different π -spacers employed in the research of organic dyes, such as pyrrole, thiazole, benzene, or thiophene [27, 32], furan has been shown to help dye stability and enhance energy conversion efficiency [36,37] due to its higher oxidation potential and lower aromatic energy.

Structural sensitizers for dye-sensitized solar cells (dssc's): dft and td-dft investigation.

Using furan as a π spacer is advised to enhance intramolecular charge transfer from donor to acceptor [27]. "Buene and co-workers found that furan performed better than popular π -spacers like thiophene" [38]. Both an electron trap and an anchor group can function as the acceptor group [14, 32]. "Due to its superior ability to withdraw electrons, cyanoacrylic acid is an excellent electron acceptor" [39] compared to other reported acceptor groups like benzothiadiazole or 2-cyano-2-pyran-4-ylideneacetic acid [27,36]. Studies have shown that density functional theory (DFT) approaches can analyze many-electron systems' electrical properties and provide ground-state properties [40-42]. The excited states of DSSC dyes have been extensively studied using this technique, both for isolated molecules and molecules coupled to a semiconductor surface [43]. Numerous studies claim that the photoelectric characteristics of different dyes can be estimated using DFT and TDDFT approaches [27].

The HOMO-LUMO gap was adjusted in this paper using the D- π -A design, with Figure 1 using the 9-vinyl-9H-carbazole (D) ring as electron donor unit and cyanoacrylic(A) inserted between various π -spacers as an "electron trap" tool to support electron transfer from the donor to the acceptor [27]. For the dye to be anchored into the semiconductor and to increase cell efficiency, cyanoacrylic acid is essential [44]. To improve the efficiency of the electron donation from the donor to the anchor group, nine (9) extra spacer units were created. To investigate how the π -spacer affects the dye's electronically characteristics and creates new dyes, each spacer unit was added at the C3 position of the carbazole ring.

Nine novel sensitizers, S1-S9, were developed in this computational work (Fig.1). According to the study, the created molecules exhibit wide visual absorption bands. Energy gap (E_g), light harvesting efficiency (LHE), open circuit voltage (V_{oc}), and frontier molecular orbital (FMO) are among the parameters that have been calculated. Our work is valuable to

effectively direct the synthesis efforts of these designed compounds (S1-S9) in the finding of high efficiency, based on the results from these factors (DSSC).

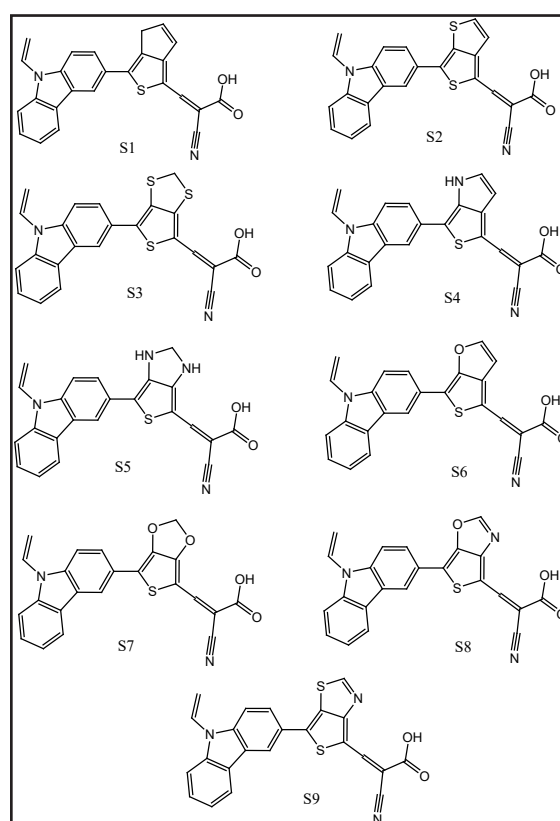


Figure 1: Molecular structure of the designed molecules (S1-S).

Materials and Methods

Computational methods

The Gaussian 09 program[45] was used to execute all calculations . Gaussian 09W is a widely used software package for performing electronic structure calculations and simulations in the field of computational chemistry. It's designed to assist researchers and scientists in exploring the properties and behavior of molecules, reactions, and materials at the quantum mechanical level. Gaussian 09W is an advanced version of the Gaussian software suite developed by Gaussian, Inc. Gaussian 09W allows research-

ers to perform a variety of quantum mechanical calculations, such as Hartree-Fock (HF), density functional theory (DFT), and post-HF methods. These calculations provide insights into molecular properties, electronic structures, and reactivity. GaussianView 5.0 is a valuable tool for researchers who perform quantum chemistry calculations using Gaussian software. It streamlines the process of job setup, result analysis, and data visualization.

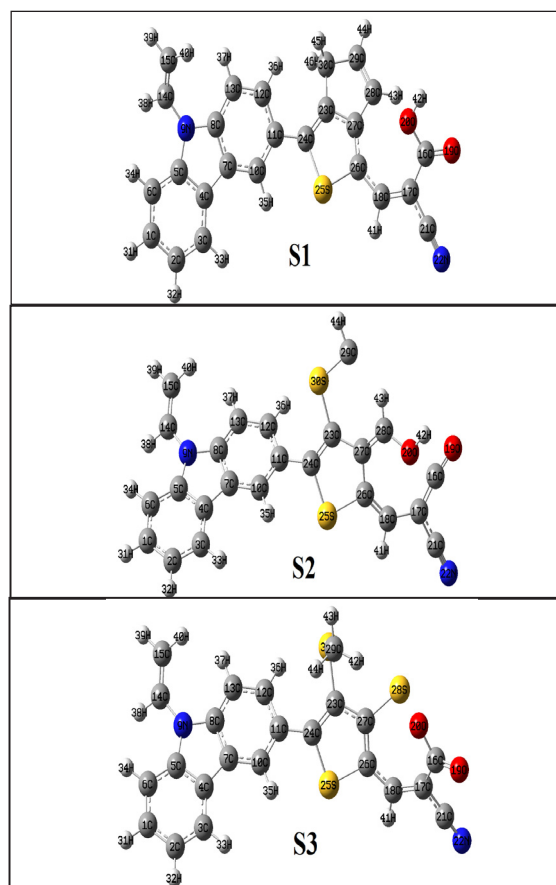
The compound's geometrical structure were optimized at the electronic ground state by DFT with B3LYP hybrid functional [46,47], using 6-311G++ basis set[48] on all atoms (C, H, O, S, N), which have been employed for theoretical analysis of organic dye for DSSC in both gas phase and solvent phase. The optimized ground state geometry was used to calculate HOMO energy, LUMO energy, and energy gap values, as well as molecular orbital distribution at frontiers. The ultraviolet-visible (UV-VIS) absorption spectra were calculated using TD-DFT at B3LYP/6-31G++ level of theory, as well as the photophysical properties such as vertical excitation energy, oscillator strength (f), and their contribution of molecular orbital responsible for the transition and percentage of composition. The solvent effect was accounted on the theoretical calculation by employing polarizable continuum model, solvent was used to dissolve molecules. When attempting to predict experimental spectra with reasonable accuracy, the incorporation of solvent influence on theoretical calculation is critical. Acetonitrile will be employed as the solvent in this study. The calculation in the solvent will be conducted by polarizable continuum model (PCM) [49-51] in the solvent phase, PCM has been used for the study of various chemical and computational calculations of the energy and electronic properties.

Results and Discussion

Geometry parameters

The most representative geometric characteristics (dihedral angle) from the op-

timized structures in Figure 2 are provided in Table 1. The elevation angle reveals the angle between two planes. The donor (D) and the π -bridge unit (π), denoted by (D- π), and the π -bridge (π) unit and acceptor unit (A), denoted by (π -A), were the dihedral angles within the optimized molecules. The dihedral angle is crucial to transmit charges within molecules [52]. To learn more about the likelihood of intramolecular charge transfer, researchers looked at the impact of the bridging unit's effect on dihedral angles. Another element that affects a molecule's stability is its dihedral angle. Table 2 lists the dihedral angles in the gas and solvent phases. Order of donor and π -bridging units (π) dihedral angles: S7>S9>S6>S1>S3>S8>S5>S4>S2 and S2~S4~S6>S8>S7>S5>S1>S3 in gas and solvent phase. Rendering to the results, S2, S3, S4 and S5 have a lower dihedral angle value



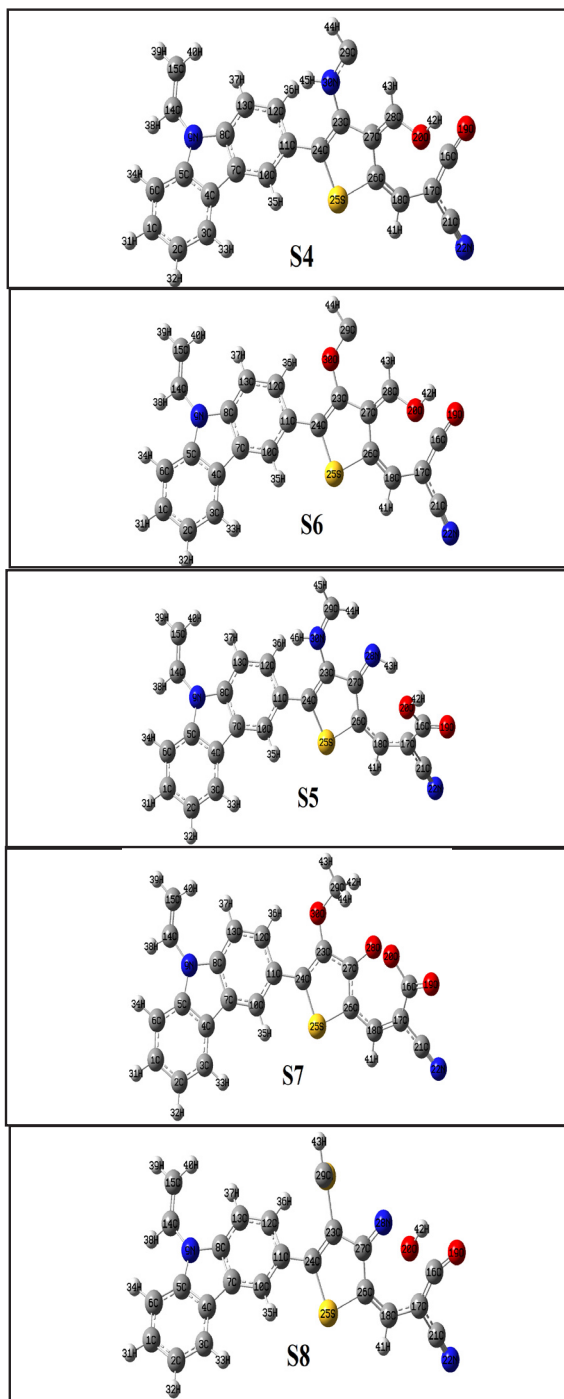


Figure 2: Geometry optimized structures of S1 to S9 dyes in the gas phase using DFT method with B3LYP functional and 6-311G++ basis set.

Table: 1. The calculated dihedral angles for donor and spacer (D- π) and spacer and acceptor (π -A) in gas and acetonitrile solvent.

| Dye | Dihedral angle | Gas | Solvent |
|-----|----------------|----------|----------|
| | | Ao | Ao |
| S1 | D- π | 155.226 | 157.988 |
| | π -A | -147.860 | -150.711 |
| S2 | D- π | -129.969 | -130.356 |
| | π -A | -179.762 | -179.844 |
| S3 | D- π | -139.725 | -139.138 |
| | π -A | -153.877 | -156.543 |
| S4 | D- π | -130.669 | -133.002 |
| | π -A | -179.707 | -179.617 |
| S5 | D- π | -135.790 | -136.008 |
| | π -A | -155.944 | -159.668 |
| S6 | D- π | -152.351 | -150.875 |
| | π -A | -179.796 | -179.641 |
| S7 | D- π | -163.804 | -164.906 |
| | π -A | -160.659 | -162.686 |
| S8 | D- π | -138.761 | -139.691 |
| | π -A | -170.084 | -166.881 |
| S9 | D- π | -158.974 | 157.881 |
| | π -A | -149.771 | -150.481 |

Frontier molecular analysis

It can be seen from an examination of the electron density distribution across the molecular orbitals in different regions of the dye under study that the ground-state dye underwent intramolecular charge transfer (ICT) (Fig. 3). The research reveals that whereas the LUMOs are dispersed among the π -spacers and the central acceptor unit, the HOMOs of molecules S2, S3, S4, S6, S7, and S5 are localized in the 9-vinyl-9H-carbazole donor group. The HOMO electrons are broadly distributed throughout the proposed molecules S9, S8, and S1, with the donor groups having the highest density and the

acceptor groups having the lowest. The number of cyanoacrylic acid units mainly determines the location of LUMOs. Dye S1–S6 has significant LUMO charge density in contrast. This shows that the injection of high electrons caused the

dye to create a semiconductor electron bond. These findings demonstrate that the (FMO) distribution is affected by the substituted-bridge groups.

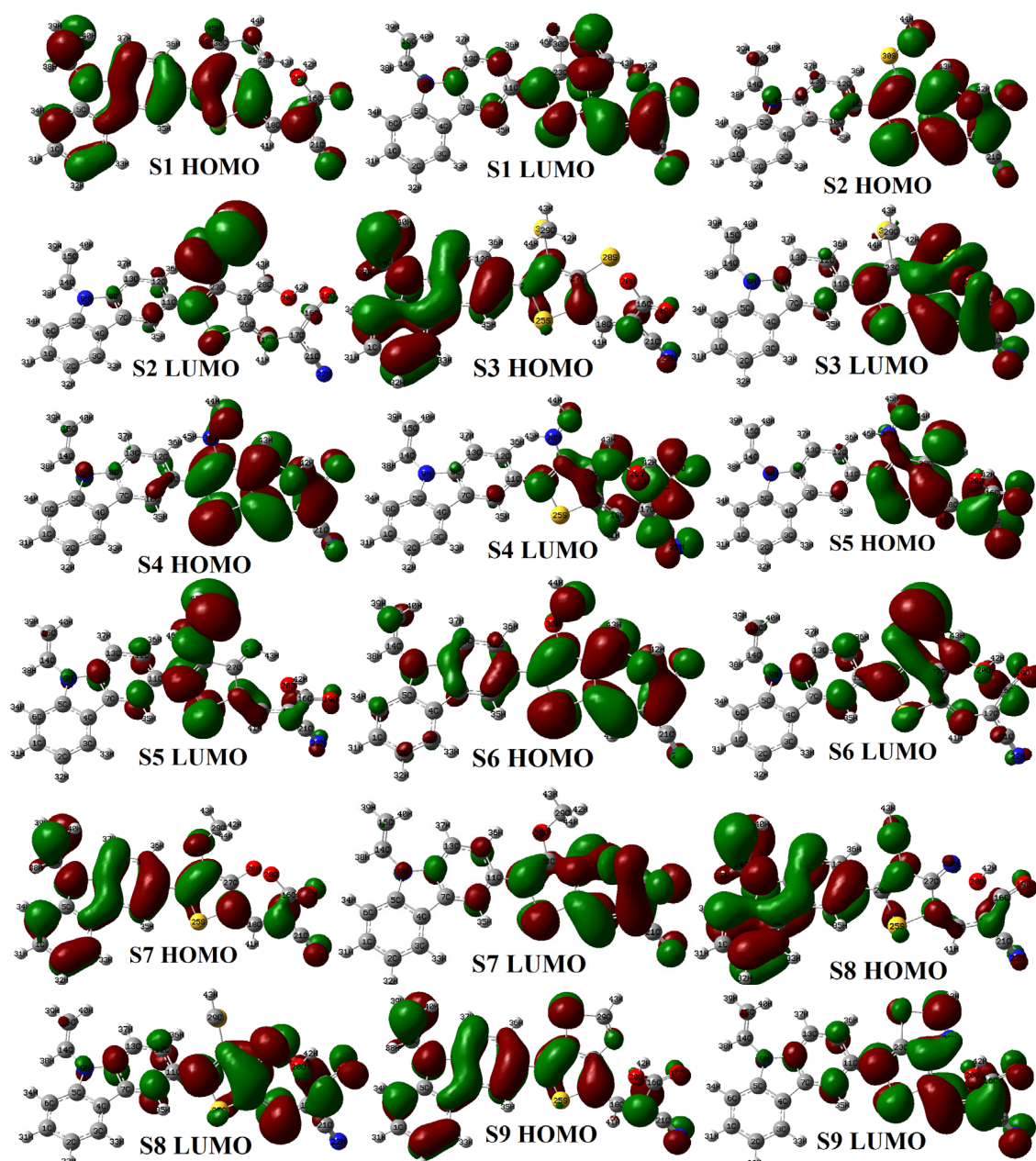


Figure 3: The HOMO and LUMO orbital diagrams for studied dyes S1 to S9 in the gas phase.

Structural sensitizers for dye-sensitized solar cells (dssc's): dft and td-dft investigation.

The optimized geometry was used to determine the E_{HOMO} , E_{LUMO} , and HOMO-LUMO energy gap (E_g) of each proposed molecule in the gas and solvent phases and Table 2 displays their values. These findings demonstrate that the density functional theory (DFT) method were wise for forecasting the newly designed molecules' photovoltaic electronic and optical properties. Furthermore, frontier molecular orbitals, also known as HOMOs and LUMOs, significantly impact electronic excitation and absorption spectra and are connected to intramolecular charge transfer, according to studies [53]. "The oxidation potential of the dye sensitizer affects the energy level of the HOMO; a high oxidation potential results in a high driving force for the reduction of the oxidized dye" [54], whereas the LUMO is electrophilic and accepts electrons. Therefore, a strong dye sensitizer typically has its HOMO mostly on the donor unit and its LUMO mostly on the acceptor unit.

Energy of HOMO-LUMO gap (E_g)

To learn about the possibility of injecting electrons into the semiconductor and regenerating the dye via the redox potential, the electronic characteristics of the improved dyes were further investigated. One key factor determining whether a dye is appropriate for DSSC application is [26]. The following equation is used to estimate the E_g values. The results are presented in Table 2.

$$E_g = E_{HOMO} - E_{LUMO} \quad (1)$$

where E_{LUMO} and E_{HOMO} are, respectively, the energies corresponding to the lowest and highest occupied molecular orbitals. A low HOMO-LUMO gap promotes a bathochromic shift and, conversely, improves the efficiency of photovoltaics [53]. Figures 4 and 5 show the HOMO and LUMO energy levels of the optimized dyes. E_g of these dyes is S1 (2.855), S2 (2.687), S3 (2.496), S4 (3.185), S5 (1.826), S6 (3.013), S7 (2.005), S8 (3.157) and S9 (2.687) in the gas phase. Dyes S5 and S7 have a low E_g of 1.8 eV and 1.7 eV in the gas and solution phases, respectively. This phenomenon caused their low

E_g ; the addition of three atoms to the -spacer unit has been noted. In addition, S5 and S7 were connected to several nitrogen and oxygen atoms with a -spacer unit.

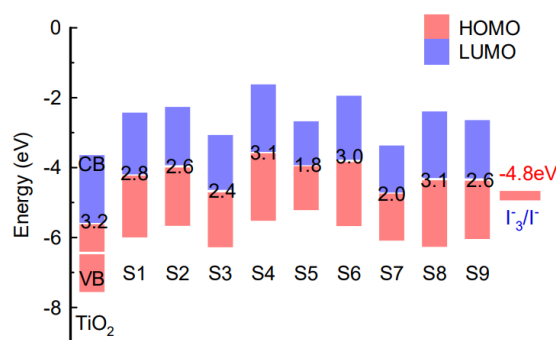


Figure 4: The energy gap (E_g) of the designed dyes S1 to S9 in the gas phase.

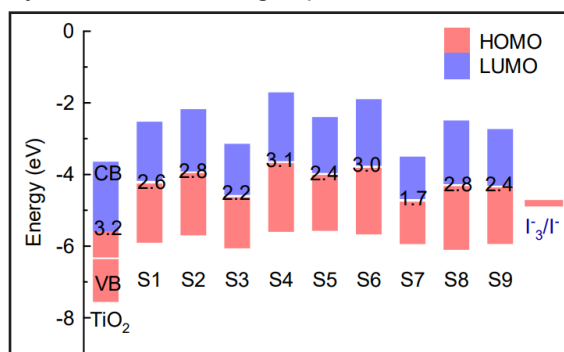


Figure 5: The energy gap (E_g) of the designed dyes S1 to S9 in a solvent.

"To improve dye recovery by stealing an electron from the electrolyte, an appropriate dye sensitizer must have a HOMO value lower than the redox potential I_3^-/I^- electrolyte, which is -4.8 eV" [55]. "Furthermore, for proper electron injection into the semiconductor's conduction band, the LUMO value of a suitable sensitizer should be above the conduction band of TiO_2 , which is -4.0 eV" [55]. This demonstrates that all computer-generated dyes can introduce electrons into TiO_2 's conduction band and then recover by collecting electrons from the electrolyte's redox potential. Furthermore, this indicates that adding various -spacer units to the D-A-based backbone significantly impacts the energy level,

which can change the absorption spectra of the simulated dyes.

UV absorption spectra

To comprehend the electronic transitions of the examined dyes, TD-DFT/B3LYP/6-311G++ computations were made and to calculate the wavelength (λ_{max}) in the gas and solvent phase. "The absorption in the visible and near ultraviolet (UV) region of the spectrum is essential for converting light into current because the improvement of absorbed dyes might likely result in good LHE" [56]. A low E_g is also required to achieve a larger max and boost DSSC effectiveness. Absorption bands with a wavelength longer than 300 nm are shown in Tables 3 and 4 as singlet-singlet transitions. The absorption wavelengths S1–S9 are 472.16, 553.46, 513.30, 557.94, 803.00, 491.27, 552.11, 914.9, 1,504.41 and 521.42, 543.81, 663.21, 549.15, 619.40, 543.88, 613.66, 759.32 and 640.98 in the gas and solvent phase respectively. The impact of the spacer unit changes the molecules' absorption spectra. The highest absorption wavelengths among the simulated dyes are S5 and S8, which increased electron delocalization and shifted the absorption band to longer wavelengths.

Table: 3. The absorption spectral transition data of the studied dyes in the gas (H=HOMO and L= LUMO).

| Dye | state | E_{exc} (eV) | λ_{max} (nm) | f | Orbital Contributions (MO) | MO% |
|-----|-------|----------------|----------------------|--------|----------------------------|-------|
| S1 | S1 | 2.6259 | 472.16 | 0.628 | H-1 -> L | 2.82 |
| | | | | | H -> L | 96.63 |
| | S2 | 3.1241 | 396.87 | 0.1616 | H-2 -> L | 19.85 |
| | | | | | H-1 -> L | 76.88 |
| | S3 | 3.2917 | 376.65 | 0.1443 | H-3 -> L | 3.87 |
| | | | | | H-2 -> L | 74.60 |
| | | | | | H-1 -> L | 17.25 |

| | | | | | | | |
|-----------|----|--------|--------|--------|-------------|-----------|-------|
| S2 | S1 | 2.2402 | 553.46 | 0.0308 | H -> L | 52.66 | |
| | | | | | H -> L +1 | 39.88 | |
| | S2 | 2.284 | 542.84 | 0.0303 | H-1 -> L +1 | 2.36 | |
| | | | | | H -> L | 44.01 | |
| | | | | | | H -> L +1 | 49.45 |
| | S3 | 2.3673 | 523.74 | 0.0072 | H-3 -> L | 32.42 | |
| H-2 -> L | | | | | 57.38 | | |
| H-1 -> L | | | | | 9.12 | | |
| S3 | S1 | 2.1626 | 573.30 | 0.1963 | H -> L | 98.83 | |
| | | | | | H-3 -> L | 10.65 | |
| | S2 | 2.572 | 482.06 | 0.0472 | H-1 -> L | 86.48 | |
| | | | | | H-4 -> L | 2.24 | |
| | S3 | 2.8053 | 441.96 | 0.0205 | H-3 -> L | 77.96 | |
| | | | | | H-2 -> L | 4.64 | |
| | | | | | H-1 -> L | 12.00 | |
| S4 | S1 | 2.2222 | 557.94 | 0.0004 | H-4 -> L | 2.61 | |
| | | | | | H-2 -> L | 2.34 | |
| | | | | | H -> L | 83.22 | |
| | | | | | H -> L +1 | 9.32 | |
| | S2 | 2.8813 | 430.31 | 0.0089 | H-1 -> L | 46.28 | |
| | | | | | H-1 -> L +1 | 47.18 | |
| | | | | | H-1 -> L +4 | 2.24 | |
| | S3 | 3.0506 | 406.43 | 0.0677 | H-1 -> L | 9.16 | |
| | | | | | H-1 -> L +1 | 8.42 | |
| | | | | | H -> L | 9.91 | |
| | | | | | H -> L +1 | 66.86 | |
| S5 | S1 | 1.5439 | 803.03 | 0.1478 | H -> L | 99.83 | |
| | | | | | H -> L +1 | 84.86 | |
| | S2 | 2.7262 | 454.79 | 0.0068 | H -> L +2 | 13.62 | |
| | | | | | H-3 -> L | 3.23 | |
| | S3 | 2.7973 | 443.23 | 0.0552 | H-2 -> L | 2.55 | |
| | | | | | H-1 -> L | 79.57 | |
| H -> L +1 | | | | | 3.75 | | |
| | | | | | H -> L +2 | 6.64 | |

| | | | | | | |
|----|----|--------|--------|--------|-------------|-------|
| S6 | S1 | 2.237 | 554.25 | 0.0009 | H -4 -> L+1 | 2.01 |
| | | | | | H -1 -> L+1 | 8.45 |
| | | | | | H->L | 13.93 |
| | | | | | H->L+1 | 70.40 |
| | S2 | 2.5237 | 491.27 | 0.0074 | H-3->L | 7.00 |
| | | | | | H-2->L | 75.31 |
| | | | | | H-2->L+1 | 7.86 |
| | | | | | H-2->L+2 | 5.96 |
| | S3 | 2.6999 | 459.21 | 0.1036 | H-1->L | 2.30 |
| | | | | | H->L | 78.15 |
| | | | | | H->L+1 | 14.07 |
| | | | | | | |

efficiency"[57];

$$\zeta = FF \frac{J_{sc} V_{oc}}{P_{inc}} \quad (2)$$

Where FF is the fill factor, Voc is open circuit voltage, Jsc is the short circuit current density and P is the intensity of the incident light. The following equation (3) is used to calculate the fill factor [10].

$$FF = \frac{I_m \times V_m}{J_{sc} \times V_{oc}} \quad (3)$$

While maximum power is connected to current and voltage, respectively (I_m and V_m), according to Eq. (3), FF, Jsc, and Voc are the significant factors influencing the photovoltaic system's photoelectric conversion efficiency. However, using Eq. (4), it is possible to determine Jsc [10].

$$J_{sc} = e \int LHE(\lambda) \phi_{inj} \eta_{reg} \eta_{cc} I_s(\lambda) d\lambda \quad (4)$$

"The LHE of dye, ϕ_{inj} , η_{reg} , and η_{cc} are used to calculate the Jsc, where ϕ_{inj} is the quantum yield of charge injection from the excited dye into the TiO₂ conduction band, reg is the regeneration efficiency, and cc is the efficiency of charge collection" [10]. Efficiency of photo-excitation and photoconversion is greatly influenced by LHE or absorbance [10]. Therefore, Eq. (5) is used to express LHE for the optimized dyes[10];

$$LHE = 1 - 0^{-f} \quad (5)$$

where f is the excited state oscillator strength corresponding to the absorption wavelength.

Through intramolecular charge transfer, high LHE is appropriate for enhancing photocurrent responsiveness [56]. The simulated dyes' LHE values are listed in Table 5. We noticed that S9 had the highest oscillator strength and the highest value of LHE (0.90). When the impact of the donor subunit is taken into account, pyrrole broadens the absorption band compared to oth-

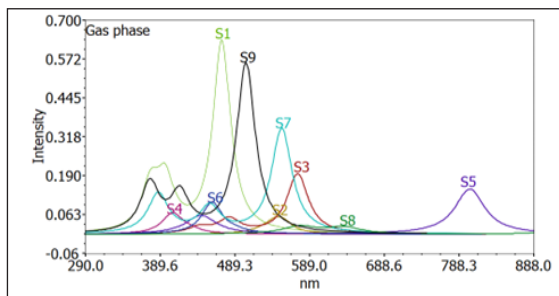


Figure 6: Calculated UV absorption spectra of the dyes in the gas phase.

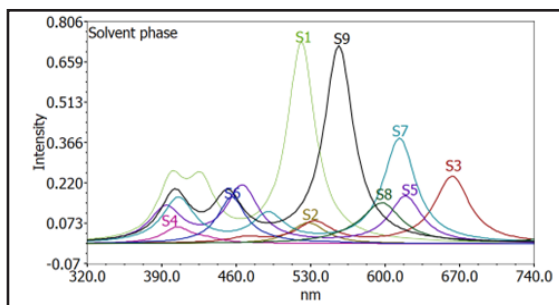


Figure 7: Calculated UV absorption spectra of the dyes in the acetonitrile solvent.

Photovoltaic properties

Eq. can be used to estimate the prediction of the overall "photoelectric conversion

er simulated dyes, improving LHE.

The V_{oc} quantifies the difference between the electrolyte's redox potential and the quasi-Fermi electron level in the TiO_2 conduction band [56]. A high V_{oc} value indicates a slower charge recombination rate [56]. The LUMOs and conduction band of the semiconductor TiO_2 are primarily responsible for a photovoltaic cell's V_{oc} . Thus, Eq. (6) and Table 5's depiction of V_{oc} provide clarification. [56]:

$$V_{OC} = E_{LUMO} - E_{CB}^{TiO_2} \quad (6)$$

According to Table 5, the dye's predicted V_{oc} values range from 0.13 to 1.74 eV. According to the V_{oc} values of S1–S9, it was evident that higher LUMO energy causes a rise in V_{oc} value, which is essential for greater photocurrent conversion efficiency in DSSCs. Furthermore, the impact of various incorporated spacer units may also be linked to variations in V_{oc} values. Given that a high V_{oc} value is better for a specific sensitizer, S6 would have the best performance in DSSC among these dyes thanks to its attractive properties and V_{oc} values of 1.69eV and 1.74 eV in the gas and solvent phases, respectively.

Table: 5. LHE and open circuit voltage (V_{oc}) in gas and acetonitrile solvent.

| dye | LHE | | VoceV | |
|-----|--------|---------|-------|---------|
| | gas | solvent | Gas | Solvent |
| S1 | 0.7645 | 0.3766 | 1.214 | 1.115 |
| S2 | 0.0685 | 0.1248 | 1.379 | 1.467 |
| S3 | 0.3636 | 0.4298 | 0.573 | 0.498 |
| S4 | 0.1443 | 0.1234 | 2.022 | 1.936 |
| S5 | 0.1443 | 0.3748 | 0.967 | 1.245 |
| S6 | 0.2122 | 0.3206 | 1.699 | 1.745 |
| S7 | 0.2583 | 0.5835 | 0.273 | 0.138 |
| S8 | 0.0553 | 0.2840 | 1.247 | 1.148 |
| S9 | 0.7218 | 0.8931 | 1.000 | 0.908 |

Conclusion

9-vinyl-9H-carbazole (D) linked to thiophene derivatives as π -spacer (π) and the D- π -A acceptor unit of cyanoacrylic acid-based dyes (A), S1 to S9, was investigated theoretically. Various π -spacers (π) were introduced at the C3 point of the 9-vinyl-9H-carbazole-based dye skeleton. The π -spacer units significantly influenced the electrical and absorption characteristics of the investigated dyes. All the studied dyes have the HOMO levels are lower than the redox potential of the electrode I/I_3^- (-4.8 eV), and the LUMO values of all optimized dyes are suitably higher than the conduction band of TiO_2 (-4.0 eV). The new dyes demonstrate an energy gap closing (3.1eV–1.1.7 eV). Due to the insertion effect of various -spacers, the S5 and S9 molecules with the lowest E_g (1.8 eV and 1.7 eV) showed the highest absorption (759 nm and 803 nm). According to this study, alterations to the reference molecules' -spacer groups impact how well the created dyes work. In conclusion, the newly designed S5 and S9 dyes are effective applications in dye-sensitized solar cells.

References

1. Hoevenaars EJ, Crawford CA. Implications of temporal resolution for modeling renewables-based power systems. *Renew Energy*. 2012;41:285-293.
2. Haradhan KM. Acid rain is a local environment pollution but global concern, *Open Sci. J Anal Chem*. 2018;3:47-55.
3. Frederica P. Pollution from fossil-fuel combustion is the leading environmental threat to global pediatric health and equity solutions exist. *Int J Environ Res Publ Health*. 2018;15(1):16.
4. Kafafy H, Wu H, Peng M, et al. Steric and solvent effect in dye-sensitized solar cells utilizing phenothiazine-based dyes. *Int J Photoenergy*. 2014;2014:1-9.
5. Sun C, Li Y, Song P, Ma F. An experimen-

- tal and theoretical investigation of the electronic structures and photoelectrical properties of ethyl red and carminic acid for DSSc application. *Materials (Basel)*. 2016;9(10):813.
6. Chen B, Yu Z, Liu K, et al. Grain engineering for perovskite/silicon monolithic tandem solar cells with efficiency of 25.4%. *Joule*. 2019;3(1):177-190.
 7. Dheivamalar S, Banu KB. A DFT study on functionalization of acrolein on Ni-doped (ZnO)₆nanocluster in dye-sensitized solar cells. *Heliyon*. 2019;5(12):e02903.
 8. El Assyry A, Lamsayah M, Warad I, Touzani R, Bentiss F, Zarrouk A. Theoretical investigation using DFT of quinoxaline derivatives for electronic and photovoltaic effects. *Heliyon*. 2020;6(3):e03620.
 9. Hagfeldt A, Boschloo G, Sun L, Kloo L, Pettersson H, Solar Cells D-S, 2010:6595-6663.
 10. Hamann TW, Jensen RA, Martinson ABF, Van Ryswyk H, Hupp JT. Advancing beyond current generation dye-sensitized solar cells. *Energy Environ Sci*. 2008;1(1):66-78.
 11. Liang M, Chen J. Arylamine organic dyes for dye-sensitized solar cells. *Chem Soc Rev*. 2013;42(8):3453-3488.
 12. Wu Y, Zhu W. Organic sensitizers from D- π -A to D-A- π -A: effect of the internal electron-withdrawing units on molecular absorption, energy levels and photovoltaic performances. *Chem Soc Rev*. 2013;42(5):2039-2058.
 13. Zhang L, Yang X, Wang W, et al.. 13.6% Efficient Organic Dye-Sensitized Solar Cells by Minimizing Energy Losses of the Excited State. *ACS Energy Lett*. 2019;4(4):943-951.
 14. O'Regan B, Grätzel M. A low-cost, high-efficiency solar cell based on dyesensitized colloidal titanium dioxide films. *Nature*. 1991;353:737-740.
 15. Semire B, Oyebamiji A, Odunola OA. Electronic properties' modulation of D-A-A via fluorination of 2-cyano-2-pyran-4-ylideneacetic acid acceptor unit for efficient DSSCs: DFT-TDDFT approach, *Scientif. Afr*. 2020;7:e00287.
 16. Arkan F, Izadyar M. The investigation of the central metal effects on the porphyrin-based DSSCs performance; molecular approach. *Mater Chem Phys*. 2017;196:142-152.
 17. Obotowo IN, Obot IB, Ekpe UJ. Organic sensitizers for dye-sensitized solar cell (DSSC): properties from computation, progress and future perspectives. *J Mol-Struct*. 2016;1122:80-87.
 18. Hua Y. Design and synthesis of new organic dyes for highly efficient dye-sensitized solar cells (DSSCs). *J Power Sources*. 2014;243:253-259.
 19. Fu JJ, Duan YA, Zhang JZ, Guo MS, Liao Y. Theoretical investigation of novel phenothiazine-based D- π -A conjugated organic dyes as dye-sensitizer in dyesensitized solar cells, *Comput. Theoret. Chem*. 2014;1045:145-153.
 20. Kumar CV, Raptis D, Koukaras EN, Sygelou L, Lianos P. Study of an indoline-phenothiazine based organic dye for dye-sensitized solar cells. Theoretical calculations and experimental data. *Org Electron*. 2015;25:66-73.
 21. Duvva N, Prasanthkumar S, Giribabu L. Influence of strong electron donating nature

- of phenothiazine on A3B- type porphyrin based dye sensitized solar cells. *Sol Energy*. 2019;184(April):620-627.
22. Slodek A, Zych D, Szafraniec-Gorol G, Gnida P, Vasylieva M, Schab-Balcerzak E. Investigations of new phenothiazine-based compounds for dye-sensitized solar cells with theoretical insight. *Materials (Basel)*. 2020;13(10).
23. Slodek A, Zych D, Golba S, Zimosz S, Gnida P, Schab-Balcerzak E. Dyes based on the D/A-acetylene linker-phenothiazine system for developing efficient dye-sensitized solar cells. *J Mater Chem C*. 2019;7(19):5830-5840.
24. Ahmad S, Guillén E, Kavan L, MGr, Grätzel M, Nazeeruddin MK. Metal free sensitizer and catalyst for dye sensitized solar cells. *Energy Environ Sci*. 2013;6(12):3439-3466.
25. Yun J-M. Materials chemistry C. *J Mater Chem* 1. 2013;3777:(207890).
26. Kacimi R, Bourass M, Toupance T, et al. Computational design of new organic (D- π -A) dyes based on benzothiadiazole for photovoltaic applications, especially dye-sensitized solar cells. *Res Chem Intermed*. 2020;46(6):3247-3262.
27. Zhang X, Gou F, Shi J, et al. Molecular engineering of new phenothiazine-based D-A- π -A dyes for dye-sensitized solar cells. *RSC Adv*. 2016;6(108):106380-106386.
28. Wu Y, Marszalek M, Zakeeruddin SM, et al. High-conversion-efficiency organic dye-sensitized solar cells: molecular engineering on D-A- π -A featured organic indoline dyes. *Energy Environ Sci*. 2012;5(8):8261-8272.
29. Wan Z, Jia C, Duan Y, Chen X, Li Z, Lin Y. Novel organic sensitizers containing dithi-fulvenyl units as additional donors for efficient dye-sensitized solar cells. *RSC Adv*. 2014;4(66):34896-34903.
30. Peng B, Yang S, Li L, Cheng F, Chen JA. Density functional theory, and time-dependent density functional theory investigation on the anchor comparison of triarylamine-based dyes. *J Chem Phys*. 2010;132:34305-34309.
31. Tan H, Pan C, Wang G, et al. A comparative study on properties of two phenoxazine-based dyes for dye-sensitized solar cells. *Dyes Pigments*. 2014;101:67-73.
32. Chermahini ZJ, Chermahini AN. Theoretical study on the bridge comparison of TiO₂ nanoparticle sensitizers based on phenoxazine in dye-sensitized solar cells. *Theor Chem Acc*. 2017;136(3):34.
33. Karlsson KM, Jiang X, Eriksson SK, et al. Phenoxazine dyes for dye-sensitized solar cells: relationship between molecular structure and electron lifetime. *Chemistry*. 2011;17(23):6415-6424.
34. Numata Y, Islam A, Chen H, Han L. Aggregation-free branch-type organic dye with a twisted molecular architecture for dye-sensitized solar cells. *Energy Environ Sci*. 2012;5(9):8548-8552.
35. Instroza N, Mendizabal F, Arratia PR, Orellana C, Linares FC. Improvement of photovoltaic performance by substituent effect of donor and acceptor structure of TPA-based dye-sensitized solar cells. *J Mol Model*. 2016;22(1):2.
36. Cariello M, Abdalhadi SM, Yadav P, et al. An investigation of the roles furan versus thiophene π -bridges play in donor- π -acceptor porphyrin based, DSSCs. *Dalton*

- Trans.* 2018;47(18):6549-6556.
37. Semire B, Oyebamiji AK, Odunola OA. Tailoring of energy levels in (2Z)-2-cyano-2-[2-[(E)-2-[2-[(E)-2-(p-tolyl)vinyl]thieno[3,2-b]thiophen-5-yl]vinyl]pyran-4-ylidene]acetic acid derivatives via conjugate bridge and fluorination of acceptor units for effective D- π -A dye-sensitized solar cells: DFT-TDDFT approach. *Res Chem Intermed.* 2017;43(3):1863-1879.
38. Buene AF, Boholm N, Hagfeldt A, Hoff BH. Effect of furan p-spacer and triethylene oxide methyl ether substituents on performance of phenothiazine sensitizers in dye-sensitized solar cells. *New J Chem.* 2019;43(24):9403-9410.
39. Hagfeldt A, Boschloo G, Sun L, Kloo L, Pettersson H. Dye-sensitized solar cells. *Chem Rev.* 2010;110(11):6595-6663.
40. Suresh T, Chitumalla RK, Hai NT, Jang J, Lee TJ, Kim JH. Impact of neutral and anion anchoring groups on the photovoltaic performance of triphenylamine sensitizers for dye-sensitized solar cells. *RSC Adv.* 2016;6(32):26559-26567.
41. Li Y, Sun C, Qi D, Song P, Ma F. Effects of different functional groups on the optical and charge transport properties of copolymers for polymer solar cells. *RSC Adv.* 2016;6(66):61809-61820.
42. Feng S, Li QS, Yang LN, Sun ZZ, Niehaus TA, Li ZS. Insights into aggregation effects on optical property and electronic coupling of organic dyes in dye sensitized solar cells. *J Power Sources.* 2015;273:282-289.
43. Nazeeruddin MK, De-Angelis F, Fantacci S, et al. atzel, Combined experimental and DFT/TDDFT computational study of photo-electrochemical cell ruthenium sensitizers. *J Am Chem Soc.* 2005;127(48):16835-16847.
44. Hua Y, Chang S, Huang D, et al. Significant improvement of dye-sensitized solar cell performance using simple phenothiazine-based dyes. *Chem Mater.* 2013;25(10):2146-2153.
45. Frisch MJ, Trucks GW, Schlegel HB, et al. Gaussian;09. Revision B.03 (Pittsburgh, PA: Gaussian Inc., 2009).
46. Lee C, Yang W, Parr RG. Development of the Colle-Salvetti correlation-energy formula into a functional of the electron density. *Phys Rev B Condens Matter.* 1988;37(2):785-789.
47. Jacquemin D, Perpète EA, Ciofini I, Adamo C. Accurate simulation of optical properties in dyes. *AccChem Res.* 2009;42(2):326-334.
48. Fan W, Chang YZ, Zhao JL, Xu ZN, Tan DZ, Chen Y. Theoretical study of fused thiophene modified anthracene-based organic dyes for dye-sensitized solar cells applications. *New J Chem.* 2018;42(24):20163-20170.
49. Bourass M, Benjelloun AT, Hamidi M, et al. re-Porte, J.M. Sotiropoulos, S.M. Bouzzine, M. Bouachrine, J. Saudi, DFT theoretical investigations of p-conjugated molecules based on thienopyrazine and different acceptor moieties for organic photovoltaic cells. *J Saudi Chem Soc.* 2013;20:415-425.
50. Lu T, Chen F. Multiwfn: a multifunctional wavefunction analyzer. *J Comput Chem.* 2012;33(5):580-592.
51. Mohajeri A, Omidvar A, Setoodeh H. Fine structural tuning of thieno[3,2-b] pyrrole donor for designing banana-shaped

- semiconductors relevant to organic field effect transistors. *J ChemInf Model.* 2019;59(5):1930-1945.
52. Prajongtat P, Suramitr S, Nokbin S, Nakajima K, Mitsuke K, Hannongbua S. Density functional theory study of adsorption geometries and electronic structures of azo-dye-based molecules on anatase TiO₂ surface for dye-sensitized solar cell applications. *J Mol Graph Model.* 2017;76:551-561.
53. Jungsuttiwong S, Tarsang R, Sudyoasuk T, Promarak V, Khongpracha P, Namuangruk S. Theoretical study on novel double donor-based dyes used in high efficient dye-sensitized solar cells: the application of TDDFT study to the electron injection process. *Org Electron.* 2013;14(3):711-722.
54. R.M. El-shishtawy, El-Shishtawy RM, Asiri AM, Aziz SG, Elroby SA. Molecular design of donor-acceptor dyes for efficient dye-sensitized solar cells I: a DFT study. *J Mol Model.* 2014;20(6):2241.
55. Fitri A, Benjelloun AT, Benzakour M, McHarfi M, Hamidi M, Bouachrine M. Theoretical investigation of new thiazolothiazole-based D- π -A organic dyes for efficient dye-sensitized solar cell. *SpectrochimActa A MolBiomolSpectrosc.* 2014;124:646-654.
56. Afolabi SO, Semire B, Akiode OK, Afolabi TA, Adebayo GA, Idowu MA. Design and theoretical study of phenothiazine-based low bandgap dye derivatives as sensitizers in molecular photovoltaics. *Opt Quantum Electron.* 2020;52(11):476.